Inverse Dopant Profiling from Transient Measurements

Marie-Therese Wolfram *

Johann Radon Institute for Computational and Applied Mathematics (ÖAW)

Altenbergerstr. 69, A-4040 Linz

wolfram.marietherese@oeaw.ac.at

Abstract

We investigate inverse problems related to the transient semiconductor device models. Our main focus is the identification of the doping profile from indirect transient measurements of electrical currents and capacitances. We present the underlying analysis and discuss the applied regularization methods. In addition, a reduced model obtained by asymptotic expansion of the drift-diffusion equations is considered, which leads to the special case of identifying piecewise constant doping profiles. Furthermore we discuss the identifiability of doping profiles and present uniqueness and non-uniqueness results for regularized solutions.

1 Introduction

The first fundamental semiconductor device model, called the drift-diffusion equations was introduced by Van Roosbroeck [16] in 1950. Today different models of various complexity exist, but the drift-diffusion equations seem to be a good compromise between efficiency and accurate description of the underlying device physics. For detailed information on the derivation of semiconductor device models and the corresponding analysis we refer to [12] and [14].

Nowadays industry is strongly interested in the identification of doping profiles for quality control purposes. Furthermore there has been a growing demand on optimizing the performance of semiconductor devices. For identification problems destructive tests, like spreading resistance profiling or non-destructive techniques, such as current, capacitance and or laser-beam-inducted current (LBIC) measurements, are used.

Identification and optimal design problems using current or capacitance measurements have been investigated concerning steady state models. There has been recent work on optimizing the performance of devices (see e.g. [11],[5]) and in identifying relevant material properties (see e.g. [3],[4],[2]). The inverse problem of reconstructing the doping profile from LBIC measurements has been considered in [2] and [8].

The main focus of this paper is the identification of the doping profile from indirect transient measurements. In steady state models current and capacitance measurements

*This work has been supported by the Austrian National Science Foundation (FWF) through project SFB F013/P1308

are taken for several applied voltages in equilibrium. In case of the transient model several measurements, taken at different time steps, are available for a single applied voltage. This significant advantage motivates the use of time dependent models for the reconstruction of the doping profile.
The transient drift-diffusion model is a system of nonlinear partial differential equations and requires consistent initial values. In practice it is assumed that a semiconductor device is at thermal equilibrium at $t = 0$, therefore we use the equilibrium solution as initial value for the transient problem. In this context we discuss inverse problems related the different measurement techniques.
The paper is organized as follows. In section 2 we introduce the transient drift-diffusion equations and discuss the underlying analysis briefly. The inverse problem of reconstructing the doping profile from indirect measurements is presented in section 3. Furthermore the adjoint approach, used for gradient evaluation is introduced shortly in section 4. The identifiability of the doping profile from indirect measurements is discussed in section 5. Finally we present solutions of computational examples in section 6.

2 The Transient Drift-Diffusion Equations

The drift-diffusion model stated on a bounded domain $\Omega \subset \mathbb{R}^d, d = 1, 2, 3$ reads as

$$\operatorname{div}(\epsilon \nabla V) = q(n - p - C) \tag{1a}$$
$$\operatorname{div} J_n = q\left(\partial_t n + R\right) \tag{1b}$$
$$\operatorname{div} J_p = q\left(-\partial_t p - R\right) \tag{1c}$$
$$J_n = q\left(D_n \nabla n - \mu_n n \nabla V\right) \tag{1d}$$
$$J_p = q\left(-D_p \nabla p - \mu_p p \nabla V\right). \tag{1e}$$

The variables are the electrical potential V ($-\nabla\ V$ denotes the electric field), the concentrations of free negatively charged carriers n (electrons) and positively charged carriers p. The predefined doping profile $C = C(x)$ of the semiconductor represents the density of implanted ions. The current densities of the holes and the electrons are denoted by J_n and J_p respectively. The total current density J is given by

$$J = J_n + J_p.$$

The parameters D_n, D_p, μ_n, and μ_p are the diffusion coefficients and mobilities of electrons and holes, respectively. In general they depend on the strength of the electric field and can be modelled by positive functions. For the sake of simplicity they are assumed to be constants in the following. Here ϵ and q are the permittivity constant and the elementary charge, which are positive constants.
The function R is the recombination-generation rate. It can be interpreted as the difference of the rate at which electron-hole carrier pairs recombine and the rate at which they are generated in the semiconductor. Several models can be found in literature, we consider the Shockley-Read-Hall (SRH) recombination-generation rate

$$R_{SRH} = \frac{np - n_i^2}{\tau_p(n + n_i) + \tau_n(p + n_i)}$$

where n_i denotes the intrinsic density and τ_n and τ_p are the lifetime of the electrons and holes respectively. Assuming that the system is in thermal equilibrium and that

the space charge (given by the right hand side of (1a)) vanishes, the Dirichlet boundary conditions can be computed as

$$\begin{aligned} n(x,t) = n_D(x) &= \frac{1}{2}(C(x) + \sqrt{C(x)^2 + 4n_i^2}) && \text{on } \partial\Omega_D \\ p(x,t) = p_D(x) &= \frac{1}{2}(-C(x) + \sqrt{C(x)^2 + 4n_i^2}) && \text{on } \partial\Omega_D \\ V(x,t) = V_D(x,t) &= U(x,t) + U_T \ln \frac{n_D(x)}{n_i} && \text{on } \partial\Omega_D, \end{aligned}$$

where U_T is the thermal voltage and $U(x,t)$ denotes the applied potential on $\partial\Omega_D$. The Neumann parts $\partial\Omega_N$ model insulating surfaces, therefore we obtain

$$\frac{\partial V}{\partial \nu} = 0 \qquad J_n(x,t)\cdot\nu = 0 \qquad J_p(x,t)\cdot\nu = 0 \qquad \text{on } \partial\Omega_N,$$

where ν denotes the unit outward normal vector on the boundary $\partial\Omega$.
Initial conditions for the free carrier concentrations n and p at the time $t = 0$ are given by

$$n(x,0) = n^I(x) \qquad p(x,0) = p^I(x) \qquad x \in \Omega.$$

Applying a suitable scaling to (1) (cf. [14]), we obtain the dimensionless formulation of the drift-diffusion equations

$$\lambda^2 \triangle V = n - p - C \tag{2a}$$
$$\partial_t n = \operatorname{div} J_n - R \tag{2b}$$
$$\partial_t p = -\operatorname{div} J_p - R \tag{2c}$$
$$J_n = \mu_n (\nabla n - n \nabla V) \tag{2d}$$
$$J_p = \mu_p (-\nabla p - p \nabla V). \tag{2e}$$

The scaled Dirichlet boundary conditions on $\partial\Omega_D$ are

$$\begin{aligned} n(x,t) = n_D(x) &= \frac{1}{2}\left(C(x) + \sqrt{C(x)^2 + 4\sigma^4}\right) \\ p(x,t) = p_D(x) &= \frac{1}{2}\left(-C(x) + \sqrt{C(x)^2 + 4\sigma^4}\right) \\ V(x,t) = V_D(x,t) &= U(x,t) + V_{bi}(x) \\ V_{bi}(x) &= \ln\left(\frac{1}{2\sigma^2}\left(C(x) + \sqrt{C(x)^2 + 4\sigma^4}\right)\right) \end{aligned}$$

and on the Neumann boundary $\partial\Omega_N$ the scaled conditions are given by

$$\frac{\partial V}{\partial \nu} = 0 \quad J_n(x,t)\cdot\nu = 0 \quad J_p(x,t)\cdot\nu = 0.$$

The parameters λ, the so-called Debye length of the device, and σ are given by:

$$\lambda = \left(\frac{\epsilon U_T}{q\tilde{C}L^2}\right)^{\frac{1}{2}} \qquad \sigma = \left(\frac{n_i}{\tilde{C}}\right)^{\frac{1}{2}}.$$

Both parameters depend on the characteristic length L of the semiconductor device and the maximum doping concentration $\tilde{C}$. For small devices and highly doped semiconductors λ tends to zero acting as a singular perturbation parameter.

2.1 The Equilibrium Case

A semiconductor device is in thermal equilibrium, if $U(x) \equiv 0$, i.e., no potentials are applied to the semiconductor contacts and $R \equiv 0$ i.e., the thermal generation is exactly balanced by recombination.
Solutions of the reduced stationary drift-diffusion equations

$$\begin{aligned} \lambda^2 \Delta V &= n - p - C \\ 0 &= \mu_n \left(\nabla n - n \, \nabla V \right) \\ 0 &= \mu_p \left(\nabla p - p \, \nabla V \right) \end{aligned}$$

are then given by

$$n = \sigma^2 e^V \qquad\qquad p = \sigma^2 e^{-V}. \tag{3}$$

The system then reduces to a nonlinear Poisson equation

$$\lambda^2 \Delta V = \sigma^2 e^V - \sigma^2 e^{-V} - C \tag{4a}$$

for the potential V with the boundary conditions

$$V(x) = V_{bi}(x) = \ln \left(\frac{1}{2\sigma^2} (C(x) + \sqrt{C(x)^2 + 4\,\sigma^4}) \right) \qquad \forall x \in \partial\Omega_D \tag{4b}$$

$$\frac{\partial V}{\partial \nu} = 0 \qquad\qquad \forall x \in \partial\Omega_N. \tag{4c}$$

In practice it is assumed that the process starts around equilibrium. Therefore n_0 and p_0 given by (3), with V_0 obtained by solving the Poisson equation (4), can be used as initial value for the time-dependent problem (2a).

2.2 Analysis of the Transient Drift-Diffusion Model

In this section we discuss existence and uniqueness results for the transient drift-diffusion model (DD-model) and specialize them to the one-dimensional case.
In [9] existence and uniqueness of global-in-time solutions for the transient drift-diffusion equations is proven. Let d denoted the space dimension and $d \leq r \leq 6$. Then under the assumption that the doping profile satisfies $C \in L^r(\Omega)$ it is shown that $(V - V_D, n - n_D, p - p_D) \in W$ where W is defined as follows:

$$W = \left\{ C([0,T]; W^2_{2,0}) \cap L^2([0,T]; W^2_{r,0}) \cap H^1([0,T]; X) \right\} \times Y \times Y,$$

with

$$\begin{aligned} Y &= C([0,T]; L^2) \cap L^2([0,T], X) \cap H^1([0,T], X^*) \\ X &= \left\{ v \in W^1_2 \mid v = 0 \text{ on } \partial\Omega_D \right\}. \end{aligned}$$

We consider the following assumptions:

(A1) $\Omega = [0,1]$;

(A2) The doping profile satisfies $C \in L^r(\Omega)$;

(A3) The mobilities satisfy $\mu_n \in L^\infty(\Omega), \mu_p \in L^\infty(\Omega)$;

(A4) The recombination-generation rate satisfies $R \in C([0,T], L^2(\Omega))$;

Note that assumption (A4) for the RSH recombination-generation rate is satisfied if $\tau_n, \tau_p \in L^\infty(\Omega)$. For the special case of spatial dimension one we are able to show higher regularity of (V, n, p).

Proposition 2.1. *Under the assumptions (A1)-(A4) stated above every solution* $(V - V_D, n - n_D, p - p_D) \in W$ *satisfies* $(V, n, p) \in \tilde{W}$ *where* $\tilde{W}$ *is defined as follows* $\tilde{W} = C([0,T], H^2(\Omega)) \times C([0,T], W^1_\infty(\Omega))^2$.

For the proof of Proposition 2.1 we refer to [17]. Furthermore in [13] it has been proven that the linearization of the drift-diffusion equations is a strongly continuous semigroup and invertible.

3 Identification of the doping profile

Inverse dopant profiling corresponds to the identification of the doping profile $C(x)$ in system (2a) from indirect measurements. The following types of measurements are used in practice:

1) *Current measurements:*
The current flow through a contact $\Gamma_1 \subset \partial\Omega_D$ is given by

$$I_{\Gamma_1}(U) = \int_{\Gamma_1} (J_n + J_p) \cdot \nu \, ds \tag{5}$$

2) *Capacitance measurements:*
The mean capacitance at a contact $\Gamma_1 \subset \partial\Omega_D$ is given by

$$\text{Cap}_{\Gamma_1}(U) = \frac{d}{dU}\left(\int_{\Gamma_1} \frac{\partial V}{\partial \nu} \, ds\right) \tag{6}$$

Note that for $\Gamma_1 = \partial\Omega$

$$\text{Cap}(U) = \frac{d}{dU}\left(\int_{\partial\Omega} \frac{\partial V}{\partial \nu} ds\right) = \frac{d}{dU}\left(\int_\Omega \Delta V \, dx\right) = \frac{d}{dU}(Q),$$

where Q denotes the total space charge.
In these cases we assume that $\Gamma_1 \subset \partial\Omega_D$ is sufficiently regular with non zero measure. A second contact is denoted by $\Gamma_2 \subset \partial\Omega_D$ with $\Gamma_1 \cap \Gamma_2 = \emptyset$. In the following we investigate whether the operators, mapping the applied potential U on Γ_2 to the current or capacitance measurements, are well-defined and continuous between appropriate spaces.

The Current-Voltage Map

The voltage current data are the measurements of the normal component of the current

density J on a contact $\Gamma_1 \subset \partial\Omega_D$ for an applied time dependent voltage $U(x,t)$. The current-voltage map is given by:

$$\begin{aligned} \Sigma_C : L^2([0,T], H^{\frac{1}{2}}(\Gamma_2)) &\to L^2([0,T]) \\ U &\mapsto I_{\Gamma_1}(U) \end{aligned} \tag{7}$$

In [17] we proof the following proposition

Proposition 3.1. *The nonlinear operator Σ_C defined by (7) is well-defined, continuous and Fréchet-differentiable.*

Capacitance Measurements

Capacitance measurements are the variation of the electric flux in normal direction on a contact Γ_1 with $U = 0$ with respect to the applied voltage U on Γ_2. The corresponding operator is given by

$$\begin{aligned} T_C : L^2([0,T], H^{\frac{1}{2}}(\Gamma_2)) &\to L^2([0,T]) \\ \phi &\mapsto \int_{\Gamma_1} \frac{\partial \hat{V}}{\partial \nu}\, ds \end{aligned}$$

where $\hat{V}$ is the solution of the linearized drift-diffusion equations around equilibrium, i.e.

$$\lambda^2 \Delta \hat{V} = \hat{n} - \hat{p} \tag{8a}$$

$$\frac{\partial \hat{n}}{\partial t} = \operatorname{div}\left(\mu_n \left(\nabla \hat{n} - \sigma^2\, e^{V_0}\, \nabla \hat{V} - \hat{n}\, \nabla V_0\right)\right) \tag{8b}$$

$$\frac{\partial \hat{p}}{\partial t} = \operatorname{div}\left(\mu_p \left(\nabla \hat{p} + \sigma^2\, e^{-V_0}\, \nabla \hat{V} + \hat{p}\, \nabla V_0\right)\right) \tag{8c}$$

with homogeneous initial conditions, homogeneous Neumann boundary conditions and the Dirichlet boundary conditions on $\partial\Omega_D$

$$\hat{V} = \phi, \quad \hat{n} = \hat{p} = 0.$$

Here V_0 denotes the solution of the Poisson equation in thermal equilibrium given by (4). We can show that the nonlinear operator T_C is well-defined, continuous and Fréchet-differentiable between suitable Sobolev spaces, see [17].
In the next sections we discuss the identification of the doping profile from either current or capacitance measurements.

3.1 Identification from Voltage-Current Data

The abstract formulation of the identification problem using current measurements is given by

$$F(C) = Y^\delta \tag{9}$$

with

$$\begin{aligned} F\colon D(F) \subset \mathcal{X} &\mapsto \mathcal{Y} \\ C &\mapsto \Sigma_C(U) \end{aligned}$$

and $\mathcal{X} = L^2(\Omega),\ \mathcal{Y} = L^2([0,T])$. The domain of the operator F is restricted to

$$D(F) = \left\{C \in H^1(\Omega) \mid \underline{C} \leq C(x) \leq \overline{C} \text{ a.e. in } \Omega\right\}$$

with positive constants $\underline{C}$ and $\overline{C}$.
Y^δ represents the noisy current data bounded by δ,i.e.

$$\left\|Y^\delta - Y\right\| \leq \delta$$

Under these assumptions we are able to verify the following result.

Proposition 3.2. *The map*

$$\begin{aligned} F\colon D(F) \subset \mathcal{X} &\to \mathcal{Y} \\ C &\mapsto \Sigma_C(U) \end{aligned}$$

is well-defined, continuous and Fréchet-differentiable. Furthermore the map F is weakly sequentially closed, i.e. for any sequence $\{C_n\} \subset D(F)$, weak convergence of C_n to $C \in \mathcal{X}$ and weak convergence of $F(C_n)$ to $y \in \mathcal{Y}$ imply that $C \in D(F)$ and $F(C) = y$.

The main idea of the proof is to rewrite the operator F as

$$\begin{aligned} F &= F_1 \circ F_2 \\ F_2 &: C \to (n, p, V) \\ F_1 &: (n, p, V) \to J \cdot \nu \end{aligned}$$

and to show that both operators are continuous and Fréchet differentiable. For further information on the proof we refer to [17].

3.2 Identification from Capacitance Measurements

Similar to the case of current-voltage data the identification problem can be written in the abstract form

$$F(C) = Y^\delta \tag{10}$$

with

$$F\colon D(F) \subset \mathcal{X} \mapsto \mathcal{Y} \tag{11}$$

$$C \mapsto T_C(U) \tag{12}$$

and $\mathcal{X} = L^2(\Omega), \mathcal{Y} = L^2([0,T])$. The domain of the operator F is the same as in the case of the voltage-current map.

Proposition 3.3. *The map*

$$\begin{aligned} F\colon D(F) \subset \mathcal{X} &\to \mathcal{Y} \\ C &\mapsto T_C(U) \end{aligned}$$

is well-defined, continuous and Fréchet-differentiable in $\mathcal{X}$. Furthermore the operator F is weakly sequentially closed.

The proof uses similar arguments as in case of current measurements, again we refer to [17] for details.

3.3 Regularization Methods

Because of the ill-posedness and the noise in the data caused by measurement errors, standard iterative methods cannot be used to solve equation (9) or (10) in a stable way. In this section regularization methods are discussed, which allow a stable solution of the inverse doping problem.
The noisy data Y^δ is bounded by δ, in case of current measurements one obtains

$$\int_0^T \left| I_{\Gamma_1}(U) - f(t) \right|^2 \, dt \leq \delta^2,$$

where $f(t)$ denotes the current measured on $\Gamma_1 \subset \partial\Omega_D$. Using capacitance measurements the assumption is given by

$$\int_0^T \left| Cap_{\Gamma_1}(U) - q(t) \right|^2 \, dt \leq \delta^2,$$

where $q(t)$ is the capacitance measured on $\Gamma_1 \subset \partial\Omega_D$.

Tikhonov Regularization

A standard regularization method for nonlinear problems is the Tikhonov regularization. Using Tikhonov regularization equation (9) is replaced by the minimization problem

$$\left\| F(C) - Y^\delta \right\|^2_{L^2([0,T])} + \alpha \left\| C - C^* \right\|^2_{L^2(\Omega)} \to \min_{C \in D(F)}, \tag{13}$$

where $\alpha > 0$, C^* is a starting value and $u = (V, n, p, V_0)$. We refer to α as the regularization parameter, which is determined by the Morozov's discrepancy principle, i.e. the largest α such that

$$\left\| F\left(C_\alpha^\delta\right) - Y^\delta \right\|_{L^2([0,T])} = \delta, \tag{14}$$

is satisfied. Here C_α^δ denotes the regularized solution, which depends on the regularization parameter α and on the noise level δ.
Since F is continuous and weakly sequentially we are able to verify the following result.

Proposition 3.4. *The minimization functional (13) admits a solution C, if F is continuous and weakly sequentially closed. Furthermore the problem has a stable dependence on the perturbed data Y^δ, i.e. if δ tends to zero the regularized solution converges to the exact solution.*

For detailed information on the proof we refer to [17], for the convergence analysis to [7].

Total Variation Regularization

Another Tikhonov-type regularization method uses the total variation of a function. This approach, introduced in [15], was originally used in image restoration, because discontinuities in the solution are preserved. Because of the discontinuity of the doping profile at the pn-junction this approach is interesting. For additional information we refer to [6, 1].
The total variation functional is defined by:

$$J_0(u) := \sup_{v \in V} \int_\Omega u \operatorname{div} v \, dx,$$

where the set of test functions is given by

$$V = \left\{ v \in C_0^\infty(\Omega)^d \mid \|g\|_\infty \leq 1 \right\}.$$

If $u \in C^1(\Omega)$ one can show, using integration by parts that

$$J_0(u) = \int_\Omega |\nabla u| \, dx \tag{15}$$

The seminorm (15) is not differentiable where $\nabla u = 0$ therefore one often considers the slightly modified functional

$$J_\beta(u) = \int_\Omega \sqrt{|\nabla u|^2 + \beta} \, dx$$

with $\beta \geq 0$. The corresponding regularized minimization problem is given by

$$\left\| F(C) - Y^\delta \right\|^2 + \alpha J_\beta(C) \to \min_{C \in D(F)}, \tag{16}$$

where α denotes the regularization parameter, determined by the discrepancy principle (14).
In [1] it is shown that a solution of the minimization problem (16) exists, if Q is weakly lower semicontinuous and BV-coercive. For both current and capacitance measurements we are able to verify the properties in an analogous to Tikhonov regularization.

4 Sensitivities

For either type of regularization method one has to solve a constrained minimization problem which can be written as

$$Q(u(C), C) \to \min_C \quad \text{subject to} \quad P(u(C), C) = 0$$

The restriction $P(u(C), C) = 0$ is the transient drift-diffusion system (2a) and the system in thermal equilibrium (4) with $u = (V, V_0, n, p)$.
In the previous section we proved that for either regularization method a minimizer exists and that all operators are continuous and Fréchet differentiable. Therefore one can use gradient based methods for minimization. The total derivative of the minimization problem can be calculated via the corresponding Lagrange functional using the adjoint equations. The Lagrange functional $\mathcal{L}$ is given by

$$\mathcal{L}(u, C, \lambda) = Q(u, C) + \langle P(u, C), \lambda \rangle.$$

Using the Kuhn Tucker restrictions

$$\frac{\partial \mathcal{L}}{\partial u}(u, C, \lambda) = \frac{\partial Q}{\partial u}(u, C) + \frac{\partial P}{\partial u}^*(u, C)\, \lambda = 0 \tag{17a}$$

$$\frac{\partial \mathcal{L}}{\partial C}(u, C, \lambda) = \frac{\partial Q}{\partial C}(u, C) + \frac{\partial P}{\partial C}^*(u, C)\, \lambda = 0 \tag{17b}$$

$$\frac{\partial \mathcal{L}}{\partial \lambda}(u, C, \lambda) = P(u, C) = 0 \tag{17c}$$

the Lagrange parameter λ can be calculated using (17a). By the chain rule the linearization of Q is given by

$$\frac{dQ}{dC} = \frac{\partial Q}{\partial u}\frac{du}{dC} + \frac{\partial Q}{\partial C} \tag{18}$$

subject to the constraint that du/dC solves the linearized equation

$$\frac{\partial P}{\partial C}\frac{du}{dC} + \frac{\partial P}{\partial C} = 0.$$

Then inserting λ into (17b) and rearranging (18) yields to

$$\frac{dQ}{dC}h = \frac{\partial \mathcal{L}}{\partial C}h \quad \forall h \in L^2.$$

Hence, the total derivative $\frac{dQ}{dC}$ can be calculated using the Fréchet derivative of the corresponding Lagrange functional $\mathcal{L}$ with respect to C.
For solving (13) or (16) we use a projected steepest descent algorithm or a projected BFGS method. In case of unipolar diodes the additional constraint that $C(x) \geq 0$ had to be satisfied.

Current Measurements

The adjoint system in case of current measurements and Tikhonov regularization is given by

$$-\lambda_1 - \frac{\partial \lambda_2}{\partial t} - \mu_n\, \Delta\lambda_2 - \mu_n\, \nabla V\, \nabla\lambda_2 + (\lambda_2 + \lambda_3)\, \frac{\partial R}{\partial n} = 0 \tag{19a}$$

$$\lambda_1 - \frac{\partial \lambda_3}{\partial t} - \mu_p\, \Delta\lambda_3 + \mu_p\, \nabla V\, \nabla\lambda_3 + (\lambda_2 + \lambda_3)\, \frac{\partial R}{\partial p} = 0 \tag{19b}$$

$$\lambda^2 \Delta\lambda_1 + \mu_n\, n\, \Delta\lambda_2 - \mu_p\, p\, \Delta\lambda_3 = 0 \tag{19c}$$

in $\Omega \times [0,T]$ and

$$\lambda^2\, \Delta\lambda_4 - \sigma^2\, \lambda_4\, (e^{V_0} + e^{-V_0}) = \sigma^2\, (\lambda_2(\cdot,0)\, e^{V_0} - \lambda_3(\cdot,0)\, e^{-V_0}) \tag{19d}$$

in Ω. The Dirichlet boundary conditions are

$$\lambda_2 = \int_{\partial\Omega} [\mu_n\, (\nabla n - n\nabla V) - \mu_p\, (\nabla p + p\, \nabla V)]\, \nu\, ds - f\,(t) \qquad \text{on } \Gamma_1 \times [0,T]$$

$$\lambda_3 = -\int_{\partial\Omega} [\mu_n\, (\nabla n - n\nabla V) - \mu_p\, (\nabla p + p\, \nabla V)]\, \nu\, ds + f\,(t) \qquad \text{on } \Gamma_1 \times [0,T]$$

$$\begin{aligned} \lambda_2 &= 0 && \text{on } \Gamma_2 \times [0,T] \\ \lambda_3 &= 0 && \text{on } \Gamma_2 \times [0,T] \\ \lambda_1 &= 0 && \text{on } \partial\Omega_D \times [0,T] \\ \lambda_4 &= 0 && \text{on } \partial\Omega_D. \end{aligned}$$

Furthermore we have homogeneous Neumann boundary conditions and the terminal conditions are given by:

$$\lambda_2(x,T) = \lambda_3(x,T) = 0 \qquad \forall x \in \Omega.$$

The partial derivative of the Lagrange functional in case of Tikhonov regularization (13) is given by

$$\frac{\partial \mathcal{L}}{\partial C}\, h_C = \int_0^T \int_\Omega \lambda_1\, h_C\, dx\, dt + \int_\Omega \lambda_4\, h_C\, dx + \alpha \int_\Omega (C - C^*)\, \nabla C\, h_C\, dx. \quad (20)$$

Capacitance Measurements

In case of capacitance measurements the adjoint system is given by

$$\lambda^2\, \Delta\lambda_1 + \mu_n\, \sigma^2\, e^{V_0}\, \Delta\lambda_2 - \mu_p\, \sigma^2\, e^{-V_0}\, \Delta\lambda_2 = 0 \quad (21a)$$

$$-\lambda_1 - \frac{\partial \lambda_2}{\partial t} - \mu_n\, \Delta\lambda_2 - \mu_n\, \nabla V_0\, \nabla\lambda_2 = 0 \quad (21b)$$

$$\lambda_1 - \frac{\partial \lambda_3}{\partial t} - \mu_p\, \Delta\lambda_3 + \mu_p\, \nabla V_0\, \nabla\lambda_3 = 0 \quad (21c)$$

and in Ω

$$\begin{aligned} &\lambda^2 \Delta\lambda_4 - \sigma^2\, e^{V_0}\lambda_4 - \sigma^2\, e^{-V_0}\lambda_4 = \\ &\int_0^T \left(-\mu_n\, \hat{n}\, \Delta\lambda_2 + \sigma^2\, e^{V_0}\, \nabla\hat{V}\, \nabla\lambda_2\right) dt + \\ &+ \int_0^T \left(\mu_p\, \hat{p}\, \Delta\lambda_3 + \sigma^2\, e^{-V_0}\, \nabla\hat{V}\, \nabla\lambda_3\right) dt + \\ &+ \lambda_2(x,0)\, \sigma^2\, e^{V_0}\, \hat{V}(x,0) - \lambda_3(x,0)\, \sigma^2\, e^{-V_0}\, \hat{V}(x,0). \end{aligned} \quad (21d)$$

The corresponding Dirichlet boundary conditions on $\partial\Omega_D = \Gamma_1 \cup \Gamma_2$,with $\Gamma_1 \cap \Gamma_2 = \emptyset$ are

$$\begin{aligned} \lambda_1 &= -\frac{1}{\lambda^2}\left(\frac{\partial \hat{V}}{\partial \nu} - q\,(t)\right) && \text{on } \Gamma_1 \times [0,T] \\ \lambda_1 &= 0 && \text{on } \Gamma_2 \times [0,T] \\ \lambda_2 &= 0 && \text{on } \partial\Omega_D \times [0,T] \\ \lambda_3 &= 0 && \text{on } \partial\Omega_D \times [0,T] \\ \lambda_4 &= 0 && \text{on } \partial\Omega_D \end{aligned}$$

Om the rest of the boundary we have homogeneous Neumann boundary conditions. Again we obtain homogenous terminal conditions for λ_2 and λ_3 instead of initial conditions. The partial derivative of the corresponding Lagrange functional with respect to C is given by

$$\frac{\partial \mathcal{L}}{\partial C}\, h_C = \int_\Omega \lambda_4\, h_C\, dx + \alpha \int_\Omega (C - C^*)\, \nabla C\, h_C\, dx. \quad (22)$$

Algorithm

From the analysis of the preceding sections we can derive the following algorithm for the minimization problem (13).

Input: initial value $C^* = C^*(x)$, applied potential $U = U(x,t)$,
measured current $f = f(t)$ or measured capacitance $q = q(t)$

(1) Solve drift-diffusion equations in thermal equilibrium (4) to obtain V_0

   (a) Solve the drift-diffusion equations (2a) for C_k to obtain (V, n, p) and calculate the total current flow J (5)

   (b) Solve the linearized drift - diffusion equations (8) to obtain $(\hat{V}, \hat{n}, \hat{p})$ and the capacitance Cap given by (6).

(2) Solve (19) and or (21) for $(\lambda_1, \lambda_2, \lambda_3, \lambda_4)$

(3) Calculate $\frac{\partial \mathcal{L}}{\partial C}(C_k)$ via (20) or (22)

(4) Determine C_{k+1} using gradient based methods such as steepest descent

(5) If convergence criterion is satisfied stop, else return to (1)

Both (2a) and (8) are systems of time dependent partial differential equations, the computation of the solutions is quite time consuming. For the reconstruction of the doping profile one can use either current measurements and/or capacitance measurements. Using both types of measurements simultaneously requires the solution of five systems of partial differential equations, first the equilibrium solution, then the drift-diffusion equations and their linearization and finally their sensitivities. This causes a high numerical effort in the reconstruction algorithm already in the one-dimensional case.

5 Non-uniqueness of Solutions

The main focus in this section is the question whether the data determines the doping profile uniquely. In mathematical terms this question is called the identifiability, which determines whether the parameter-to-output map F is injective. We furthermore present numerical examples to illustrate the numerical difficulties.
Gajewski proved in [9] that for the transient drift-diffusion equations a unique solution exists. Uniqueness results were presented in the steady state case under the assumption that the applied voltage is small (see [3]).
In [3] it is shown that in one dimension the doping profile of a unipolar diode can be identified uniquely from a single transient measurement. But for this result additional smoothness assumptions are required: The doping profile is assumed to be a continuously differentiable function whose partial derivatives are Hölder continuous with H"/older exponent $\alpha = 1$, i.e. $C \in C^{1,1}(\Omega)$. In case of discontinuous doping profiles these results do not apply.
So far there has been no results on the unipolar multi-dimensional inverse doping problem. For more general devices like np-diodes no uniqueness results have been derived yet.
Throughout this section only the one-dimensional case is considered and the following assumptions are made:

- The mobilities of the electrons and holes are equal, i.e. $\mu_n = \mu_p$.
- The relaxation times of the electrons and holes are equal, i.e. $\tau_n = \tau_p$.

Under these assumptions we can show that the inverse problem for the drift-diffusion equations, considering both current and capacitance measurements admits at least two solutions.

Proposition 5.1. *There exist at least two solutions $C_i \in H^1(\Omega)$, $i = 1, 2$ to the inverse problem for the drift-diffusion equations (2a). In particular, if (n_1, p_1, V_1, C_1) is a solution of (2a) there exists a second solution (n_2, p_2, V_2, C_2) given by*

$$C_2(x) = -C_1(1-x), \tag{23a}$$
$$n_2(x,t) = p_1(1-x,t), \tag{23b}$$
$$p_2(x,t) = n_1(1-x,t), \tag{23c}$$
$$V_2(x,t) = -V_1(1-x,t) + U(x,t), \tag{23d}$$

such that

$$J_{n_2} = J_{p_1}, \quad J_{p_2} = J_{n_1}$$
$$Cap\,(V_2) = Cap\,(V_1).$$

For details on the proof we refer to [17].
We consider Tikhonov regularization and obtain the minimization problem

$$Q_f(u,C) = |F(C) - f(t)|^2 + \alpha\,|C - C^*|^2 \to \min_C \tag{24}$$

where $f(t)$ denotes the current measurements or

$$Q_q(u,C) = |F(C) - q(t)|^2 + \alpha\,|C - C^*|^2 \to \min_C \tag{25}$$

where $q(t)$ refers to the capacitance measurements. The operator F maps the doping profile C either to the current or to the capacitance measured at a contact Γ_1. In both cases the weak sequential closedness of F, see Proposition 3.2, ensures the existence of a solution for both minimization problems. Under the assumptions made above it has already been shown that the inverse problem admits multiple solutions, therefore one cannot expect unique minimizers of both functionals.
Indeed it is possible to construct cases where the multiple solutions are both minimizers of (24) and (25).

Proposition 5.2. *Let the assumptions of Proposition 5.1 and*

$$C^*(x) = -C^*(1-x).$$

hold. Then there exist at least two minimizers of the optimization problem (24) and (25). The multiple solutions of the inverse problem given by (23) are minimizers of the Tikhonov functionals (24) and (25). Furthermore

$$Q_f(n_1, p_1, V_1, C_1) = Q_f(n_2, p_2, V_2, C_2)$$
$$Q_q(n_1, p_1, V_1, C_1) = Q_q(n_2, p_2, V_2, C_2)$$

holds.

For the proof of the proposition we refer to [17]. In case of total variation regularization one can show similar results.
We mention that our analysis of multiple solutions was motivated by similar results

concerning the steady state DD-model (cf. [10]). Considering a slightly different minimization functional one could avoid the existence of the multiple solutions constructed above. This functional is given by:

$$Q(u,C) = \int_0^T \left| \int_{\Gamma_1} J_n \, d\nu - f_n(t) \right|^2 dt + \int_0^T \left| \int_{\Gamma_1} J_p \, d\nu - f_p(t) \right|^2 dt + \\ + \alpha \int_\Omega \mid C - C^* \mid^2 dx. \tag{26}$$

For (26) the couple (n_2, p_2, V_2, C_2) constructed in (23) is not a minimizer any more. This provides reasonable remedy for optimal design and optimal control tasks as considered in [10], but for the identification of the doping profile this means that one has to measure the current caused by the holes and the current caused by the electrons separately, which is not possible in practice !

6 Numerical examples

In this section we present results of computational examples in case of one-dimensional unipolar diodes . All computations have been performed on the software systems MATLAB 7 and FEMLAB 3.1.
In our examples we used typical values of the parameters of silicon at room temperature $(T = 300K)$, listed in Table 1.

Parameter	Physical Meaning	Numerical Value
q	elementary charge	$1.6 \cdot 10^{-19}$ As
n_i	intrinsic density	10^{10} cm^{-3}
ϵ_S	permittivity constant	10^{-12} As V^{-1}s^{-1}
μ_n	mobility of electrons	$1.5 \cdot 10^3$ cm^{2}V^{-1}s^{-1}
μ_p	mobility of holes	10^3 cm^{2}V^{-1}s^{-1}
U_T	thermal voltage	0.0259 V
τ_n	lifetime of electrons	10^{-6} s
τ_p	lifetime of holes	10^{-5} s

Table 1: Physical parameters for silicon at room temperature

To generate artificial measurement data, we solved the direct problem (2a) for an applied voltage U and a given doping profile C. The forward problem was solved on a regular mesh with 800 nodes, using a piecewise linear finite element base. In order to avoid an inverse crime we used a different sized mesh for the evaluation of the gradient of (13) or (16).

6.1 n-Diode

The simplest semiconductor device is a one-dimensional unipolar diode. The exact doping profile is given by

$$C(x) = \begin{cases} 1 & 0 \leq x \leq 0.5, \\ 0 & 0.5 < x \leq 1. \end{cases}$$

The drift-diffusion system (2a) and the sensitivities (19) are solved on a regular mesh of 240 nodes. We choose a diode of length $L = 10^{-4}$ cm and a maximum doping concentration of $\tilde{C} = 10^{16}\,\mathrm{cm}^{-3}$.
The applied voltage is

$$U(x,t) = 10^{-5}(t + \sin(t)).$$

For the applied time scaling we obtain

$$t = \frac{L^2}{U_T \tilde{\mu}} t_s = \frac{1e^{-8}}{1e^{-2}} t_s = 1e^{-6} s.$$

Solving the DD-model over a large time interval $[0 : 100\ s : 10000\ s]$ seems to be a realistic setup.
Reconstructions have been performed using a projected steepest descent or a projected BFGS algorithm with the constraint

$$C(x) \geq 0.$$

Figure 1(a) shows the reconstructed doping profile of a unipolar diode using steepest descent algorithm and Tikhonov regularization. The evaluation of the corresponding cost function is given in Figure 1(b). After 30 iterations a regularized solution is obtained, the corresponding value of Q is 10^{-6}.

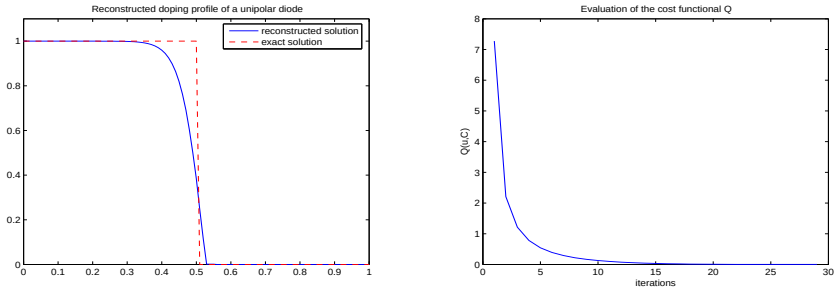

(a) Reconstructed doping profile

(b) Evaluation of the cost functional Q

Figure 1: Reconstructed doping profile using current measurements and Tikhonov regularization

In Figure 2(a) and 2(b) we see the regularized solution and the corresponding cost functional Q using total variation regularization, with $\beta = 10^{-5}$.The solution is similar

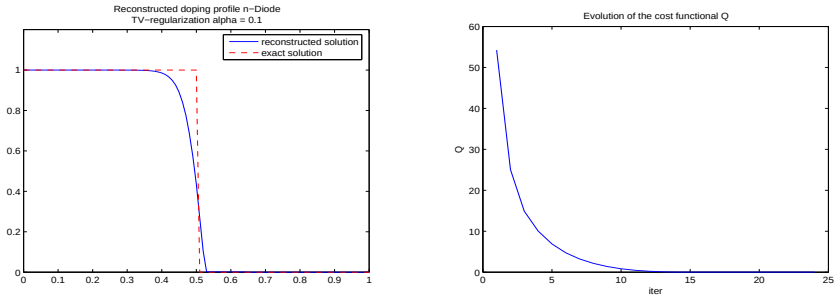

(a) Reconstructed doping profile (b) Evaluation of the cost functional Q

Figure 2: Reconstructed doping profile using current measurements and TV regularization

to the one obtained by Tikhonov regularization, but the gradient of the doping profile is steeper around the junction.

In case of noisy data the choice of the regularization parameter is important for the quality of the regularized solution. According to the discrepancy principle (14) we choose the regularization parameter such that

$$\delta \leq \left| F(C) - Y^{\delta} \right| \leq \tau \, \delta \tag{27}$$

with $\tau = 1.1$.
Figure 3(a) shows the regularized solution for the noise level $\delta = 5\%$.

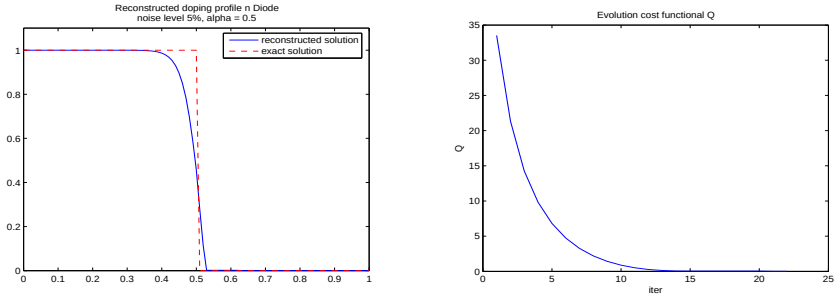

(a) Reconstructed doping profile (b) Evaluation of the cost functional Q

Figure 3: Reconstructed doping profile using current measurements with $\delta = 5\%$

6.2 $\mathrm{n^+nn^+}$ Diode

A $\mathrm{n^+nn^+}$ Diode is the combination of a highly doped n-region, a lower doped n-region and another higher doped n-region. The corresponding doping profile is given by:

$$C(x) = \begin{cases} 1 & 0 \leq x \leq 0.3 \\ 0.1 & 0.3 < x < 0.7 \\ 1 & 0.7 < x \leq 1. \end{cases}$$

We started with a good initial guess

$$C^*(x) = \begin{cases} 1 & 0 \leq x \leq 0.3 \\ 0.2 & 0.3 < x < 0.7 \\ 1 & 0.7 < x \leq 1. \end{cases}$$

The value of the applied potential was the same as in the case of a unipolar diode. Because of the two jumps we used a finer mesh with 480 nodes. After three iterations the reconstruction stopped because the calculated gradient yielded no descent direction. Figure 4(a) shows the reconstructed doping profile after 3 iterations, Figure 4(b) the gradient evaluation for this doping profile.
In the case of capacitance measurements such issues do not occur. The parameters are the same as in the case of current measurements. The reconstruction from capacitance measurements is more time consuming than in case of current measurements due to the numerical integration of the right hand side of equation (21d). The reconstructed doping profile and the evolution of the cost functional can be seen in Figure 5(a) and Figure 5(b).

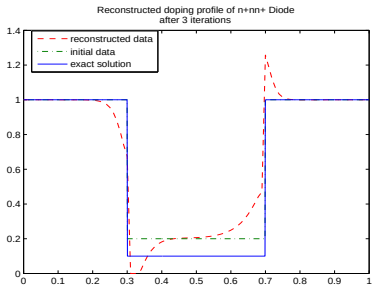

(a) Reconstructed doping profile

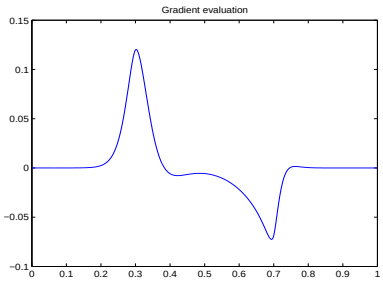

(b) Gradient after 3 iterations

Figure 4: Reconstructed doping profile after 3 iterations using current measurements

6.3 np-Diodes

In this section we present numerical examples, which illustrate the difficulties that arise due to the non-uniqueness of the regularized solution. We used a finer mesh with 1000

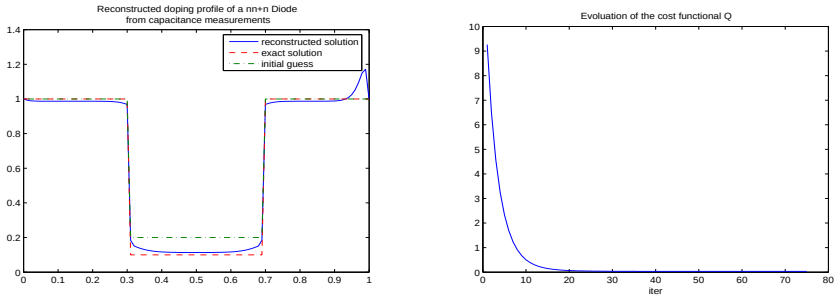

(a) Reconstructed doping profile (b) Evaluation of the cost functional Q

Figure 5: Reconstructed doping profile using capacitance measurements

nodes to generate data and 840 nodes to evaluate the gradient of the minimization functional.
We consider a semiconductor device of length $L = 10^{-4}$ cm and a maximum doping concentration $\tilde{C} = 10^{16}$ cm^{-3}. Setting $\tau_n = \tau_p = 1e^{-6}$ and $\mu_n = \mu_p = 1000$ allows the existence of multiple solutions as described in Section 5.
The exact doping profile is given by

$$C(x) = \begin{cases} 1 & 0 \leq x \leq 0.5 \\ -0.5 & 0.5 < x \leq 1 \end{cases}$$

the initial guess by

$$C^*(x) = \begin{cases} 1 & 0 \leq x \leq 0.5 \\ -0.3 & 0.5 < x \leq 1. \end{cases}$$

In Figure 6(a) the two possible solutions that produce the same total current are illustrated. In Figure 6(b) the gradient of the initial guess is shown - this gradient would be a steepest descent direction for the second solution, but not for the first one.

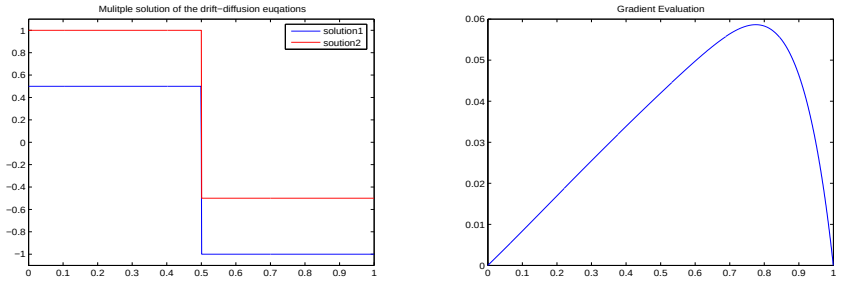

(a) Possible multiple solutions (b) Gradient Evaluation

Figure 6: Multiple solution in case of a np-diode

In the second example we set $\mu_n = 1500$ and $\mu_p = 1000$. Furthermore when considering the symmetric doping profile

$$C(x) = \begin{cases} 1 & 0 \le x \le 0.5 \\ -1 & 0.5 < x \le 1 \end{cases}$$

the two possible solutions are identical. In this case we could reconstruct the doping profile using Tikhonov regularization. The reconstructed solution is displayed in Figure 7(a) and the corresponding cost functional Figure 7(b).

After 90 iterations (about 4 hours) the regularized solution was obtained. The results

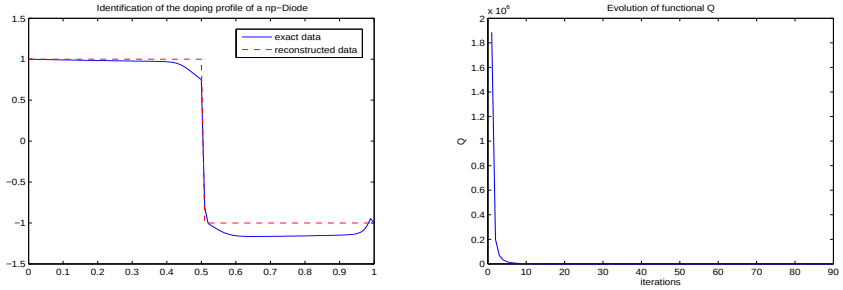

(a) Reconstructed doping profile

(b) Evaluation of the cost functional Q

Figure 7: Reconstructed doping profile using current measurements

are very satisfactory, due to regularization the reconstructed solution is smoother than the exact one.

References

[1] R. ACAR AND C. R. VOGEL, *Analysis of bounded variation penalty methods for ill-posed problems*, Inverse Problems, 10 (1994), pp. 1217–1229.

[2] M. BURGER, H. W. ENGL, A. LEITAO, AND P. A. MARKOWICH, *On inverse problems for semiconductor equations*, Milan J. Math., 72 (2004), pp. 273–313.

[3] M. BURGER, H. W. ENGL, AND P. A. MARKOWICH, *Inverse doping problems for semiconductor devices*, in Recent progress in computational and applied PDEs (Zhangjiajie, 2001), Kluwer/Plenum, New York, 2002, pp. 39–53.

[4] M. BURGER, H. W. ENGL, P. A. MARKOWICH, AND P. PIETRA, *Identification of doping profiles in semiconductor devices*, Inverse Problems, 17 (2001), pp. 1765–1795.

[5] M. BURGER AND R. PINNAU, *Fast optimal design of semiconductor devices*, SIAM J. Appl. Math., 64 (2003), pp. 108–126 (electronic).

[6] D. DOBSON AND O. SCHERZER, *Analysis of regularized total variation penalty methods for denoising*, Inverse Problems, 12 (1996), pp. 601–617.

[7] H. W. ENGL, M. HANKE, AND A. NEUBAUER, *Regularization of inverse problems*, vol. 375 of Mathematics and its Applications, Kluwer Academic Publishers Group, Dordrecht, 1996.

[8] W. FANG AND K. ITO, *Reconstruction of semiconductor doping profile from laser-beam-induced current image*, SIAM J. Appl. Math., 54 (1994), pp. 1067–1082.

[9] H. GAJEWSKI, *On existence, uniqueness and asymptotic behavior of solutions of the basic equations for carrier transport in semiconductors*, Z. Angew. Math. Mech., 65 (1985), pp. 101–108.

[10] M. HINZE AND R. PINNAU, *Multiple solutions to a semiconductor design problem*, tech. rep., TU Dresden.

[11] ——, *An optimal control approach to semiconductor design*, Math. Models Methods Appl. Sci., 12 (2002), pp. 89–107.

[12] P. A. MARKOWICH, *The stationary semiconductor device equations*, Computational Microelectronics, Springer-Verlag, Vienna, 1986.

[13] P. A. MARKOWICH AND C. A. RINGHOFER, *Stability of the linearized transient semiconductor device equations*, Z. Angew. Math. Mech., 67 (1987), pp. 319–332.

[14] P. A. MARKOWICH, C. A. RINGHOFER, AND C. SCHMEISER, *Semiconductor equations*, Springer-Verlag, Vienna, 1990.

[15] L. RUDIN, S. OSHER, AND E. FATEMI, *Nonlinear total variation based noise removal algorithms*, Physica D: Nonlinear Phenomena, (1992), pp. 259–268.

[16] W. VAN ROOSBROECK, *Theory of the flow of electrons and holes in germanium and other semiconductors*, Bell Syst. Tech. J., (1950), pp. 560–607.

[17] M.-T. WOLFRAM, *Semiconductor inverse dopant profiling from transient measuremenst*, Master's thesis, Johannes Kepler University Linz, 2005.